

GA-A27412

**ACCESS AND SUSTAINED HIGH PERFORMANCE IN
ADVANCED TOKAMAK INDUCTIVE DISCHARGES
WITH ITER-RELEVANT LOW TORQUE**

by

W.M. SOLOMON, P.A. POLITZER, R.J. BUTTERY, J.R. FERRON, A.M. GAROFALO,
B.A. GRIERSON, J.M. HANSON, Y. IN, G.L. JACKSON, C.T. HOLCOMB, J.E. KINSEY,
R.J. LA HAYE, M.J. LANCTOT, T.C. LUCE, M. OKABAYASHI, C.C. PETTY, F. TURCO,
and A.S. WELANDER

OCTOBER 2012



DISCLAIMER

This report was prepared as an account of work sponsored by an agency of the United States Government. Neither the United States Government nor any agency thereof, nor any of their employees, makes any warranty, express or implied, or assumes any legal liability or responsibility for the accuracy, completeness, or usefulness of any information, apparatus, product, or process disclosed, or represents that its use would not infringe privately owned rights. Reference herein to any specific commercial product, process, or service by trade name, trademark, manufacturer, or otherwise, does not necessarily constitute or imply its endorsement, recommendation, or favoring by the United States Government or any agency thereof. The views and opinions of authors expressed herein do not necessarily state or reflect those of the United States Government or any agency thereof.

ACCESS AND SUSTAINED HIGH PERFORMANCE IN ADVANCED TOKAMAK INDUCTIVE DISCHARGES WITH ITER-RELEVANT LOW TORQUE

by

W.M. SOLOMON,* P.A. POLITZER, R.J. BUTTERY, J.R. FERRON, A.M. GAROFALO,
B.A. GRIERSON,* J.M. HANSON,[†] Y. IN,[‡] G.L. JACKSON, C.T. HOLCOMB,[#] J.E. KINSEY,
R.J. LA HAYE, M.J. LANCTOT,[#] T.C. LUCE, M. OKABAYASHI,* C.C. PETTY, F. TURCO,[†]
and A.S. WELANDER

This is a preprint of a paper to be presented at the Twenty-fourth
IAEA Fusion Energy Conf., October 8-13, 2012 in San Diego,
California.

*Princeton Plasma Physics Laboratory, Princeton, New Jersey, USA.

[†]Columbia University, New York, New York, USA.

[‡]FAR-TECH, Inc., San Diego, California, USA.

[#]Lawrence Livermore National Laboratory, Livermore, California, USA.

Work supported in part by
the U.S. Department of Energy
under DE-AC02-09CH11466, DE-FC02-04ER54698,
DE-FG02-08ER85195, and DE-AC52-07NA27344

GENERAL ATOMICS PROJECT 30200
OCTOBER 2012

Access and Sustained High Performance in Advanced Inductive Discharges with ITER-Relevant Low Torque

W.M. Solomon 1), P.A. Politzer 2), R.J. Buttery 2), J.R. Ferron 2), A.M. Garofalo 2), B.A. Grierson 1), J.M. Hanson 3), Y. In 4), G.L. Jackson 2), C.T. Holcomb 5), J.E. Kinsey 2), R.J. La Haye 2), M.J. Lanctot 5), T.C. Luce 2), M. Okabayashi 1), C.C. Petty 2), F. Turco 3), and A.S. Welander 2)

- 1) Princeton Plasma Physics Laboratory, Princeton, New Jersey 08543-0451, USA
- 2) General Atomics, PO Box 85608, San Diego, California 92186-5608, USA
- 3) Columbia University, New York, New York 10027, USA
- 4) FAR-TECH, Inc., 10350 Science Center Dr., San Diego, California 92121-1136, USA
- 5) Lawrence Livermore National Laboratory, Livermore, California 94551, USA

e-mail contact of main author: solomon@fusion.gat.com

Abstract. Recent experiments on DIII-D have demonstrated that advanced inductive discharges with high normalized fusion gain approaching levels consistent with ITER $Q=10$ operation can be accessed and sustained with very low amounts (~ 1 Nm) of externally driven torque. The advanced inductive regime is typically characterized by high confinement, and high β_N operation, allowing the possibility for operation at lower plasma current, and these present experiments use a level of torque that is anticipated to drive a similar amount of rotation as the beams on ITER, via simple consideration of the scaling of the moment of inertia and confinement time. These discharges have achieved $\beta_N \sim 3.1$ with $H_{98} \sim 1$ at $q_{95} \sim 4$, and have been sustained for the maximum duration of the counter neutral beams (NBs). In addition, plasmas using zero net neutral beam torque from the startup all the way through to the high β phase have been created. Advanced inductive discharges are found to become increasingly susceptible to 2/1 neoclassical tearing modes as the torque is decreased, which if left unmitigated, generally slow and lock, terminating the high performance phase of the discharge. Access is not notably different whether one ramps the torque down at high β_N , or ramps the β_N up at low torque. The use of electron cyclotron heating (ECH) and current drive (ECCD) has proven to be an effective method of avoiding such modes, enabling the stable operation at high beta and low torque, a portion of phase space that has otherwise been inaccessible. In many cases, the ECH has been aimed to drive current near the $q=2$ surface, although it is not clear that this is a critical element to gain the benefits of the ECH. Indeed, high $\beta_N \sim 3$ discharges at low torque have been sustained using ECH without current drive, and deposited significantly inside of the $q=2$ surface. The insensitivity to the deposition position, together with the lack of need for current drive, suggests that the EC assists stability in a different way than simply replacing the bootstrap current caused by the flattening of the pressure profile in the island. These advanced inductive discharges are measured to have significant levels of intrinsic torque at the edge, consistent with a previously determined empirical scaling considering the role of the turbulent Reynolds stress and thermal ion orbit loss.

1. Introduction

High performance regimes in tokamaks are typically produced with high levels of externally driven torque from neutral beams, and consequent rapid toroidal rotation. Significant toroidal rotation has been shown to be beneficial to plasma performance, both in terms of stability [1] and confinement [2], but the ability to drive such rotation in ITER and future burning plasmas is unclear, due to the plasma's rapid increase in moment of inertia with machine size compared with the confinement time. Whilst the effect of rotation on scenarios such as the advanced inductive (AI) and "hybrid" regime has previously been studied [3], such research has generally been done by first initiating the high performance state with high torque and later ramping the torque down. Hence, an outstanding issue is whether high torque is a requirement for accessing the advanced inductive scenario (or indeed all regimes). In this paper, we investigate the performance, confinement and stability of advanced inductive plasmas produced with low torque through to the high beta phase. The advanced inductive scenario offers a potentially attractive alternative operating mode for ITER [4,5]. It is typically characterized by high confinement, which, when coupled with high β_N operation,

allows the possibility for operation at lower plasma current, with lower associated risk to the machine from high current disruptions, while still reaching $Q=10$ mission.

The data in Fig. 1 summarizes the challenges in producing high performance plasmas at low rotation, which shows a typical advanced inductive discharge initiated with high torque, followed by a torque ramp to near balanced neutral beam injection. The plasma stored energy is maintained during this torque ramp using β_N -feedback control of the neutral beam power. One immediately notices that the power demand for the fixed β_N target goes up by 70%, and the H-mode confinement quality, characterized by H_{98} , is reduced from about 1.5, indicating excellent core confinement, to just above 1 (closer to standard H-mode performance). This dynamic response is similar to a database of stationary advanced inductive discharges run with varying levels of torque [3]. Typically, one sees that the 3/2 NTM amplitude doubles during such torque ramps, which may account for perhaps 10% of the loss in confinement. Perhaps most problematic, toward the end of the torque ramp, an unmitigated $m/n = 2/1$ neoclassical tearing mode (NTM) is triggered, which terminates the high performance phase of the discharge.

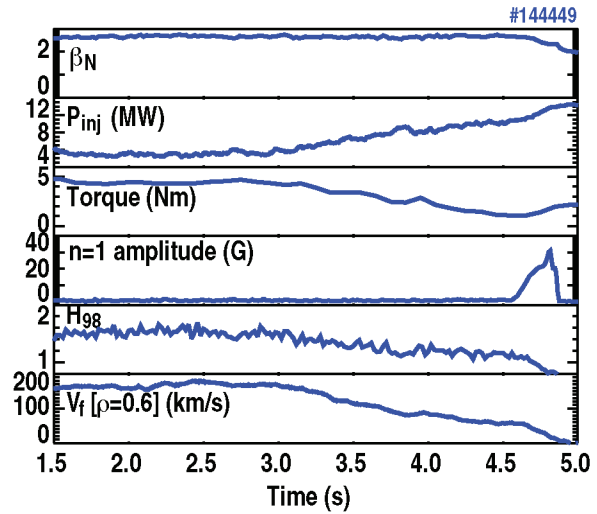


FIG. 1. Time history of typical advanced inductive discharge with a NBI torque ramp-down, in this case ending with a 2/1 NTM. (a) β_N , (b) injected beam power, (c) NBI torque, (d) $n=1$ mode amplitude, (e) H_{98} confinement factor and (f) toroidal velocity near $q=2$.

2. Stability Properties of Low Torque Advanced Inductive Plasmas

A commonly observed characteristic of high β advanced inductive plasmas is the existence of (normally) relatively benign 4/3 or 3/2 NTMs. The island width of such modes has previously been found to increase as the rotation is reduced [3], and since the torque exerted by the mode on the plasma grows with the mode size [6], this sets up a positive feedback loop. As a result, it is often the case that when the torque is ramped down, the 3/2 mode grows, and either locks to the wall, or more commonly, a 2/1 NTM is destabilized and rapidly locks. Typically, this occurs in advanced inductive plasmas with $\beta_N > 2.5$ and low torque $T < 1$ Nm. Previous experiments have shown that electron cyclotron current drive (ECCD) aimed accurately at the appropriate resonant surface can stabilize both 3/2 [7] and 2/1 [8] NTMs. The first efforts to explore lower torque advanced inductive operation had attempted to short-circuit the positive feedback loop by attempting to either suppress or maintain the size of the 3/2 mode using ECCD. However, it was generally the case that a 2/1 NTM would nonetheless be triggered at about the same level of rotation and torque. The more recent experiments re-aimed the EC power to broadly deposit near the $q=2$ surface (typically around $\rho \sim 0.5-0.6$). This successfully opened up operation to very low torque levels, all the way to balanced injection (0 Nm).

Indeed, plasmas using zero net neutral beam torque from the startup through the high β phase have been created, using only modest amounts of EC power (~ 1 MW). At this power level, the 2/1 NTM could be limited in size sufficiently (though still appreciable in magnitude, $|\tilde{B}_\theta| \approx 12$ G) to allow stable operation at $\beta_N \sim 2.5$, limited by confinement (clearly impacted by the presence of a large 2/1 NTM) and the available balanced NB power. Figure 2 shows that the discharge maintains fairly stationary conditions for approximately 1 s, during

which time the rotation frequency is very low (~ 1 kHz), and remarkably flat across most of the profile. The drag exerted on the plasma by this sizeable NTM with the resistive wall eddy currents, can be estimated, $d\omega/dt = C_w^{-1} \tau_A^{-2} (m\omega\tau_w)(w/a)^4$ [4], where $C_w \sim 14$ [9], τ_A the Alfvén time, τ_w the wall time, ω the toroidal rotation, and w is the island width. The seed island width is given by $w \approx (2/3)(16r_s R_0 |\tilde{B}_r|^2) / (msB_\phi)$ [10], where r_s is the minor radius of the surface and $s = r(dq/dr)q^2$ and the radial field at the mode is related to the measured poloidal field at the wall by $|\tilde{B}_r| \approx 0.5(b/r_s)|\tilde{B}_\theta|_{\text{wall}}$. For these conditions, the island is estimated to grow to approximately 10 cm (nearly 20% of the minor radius), and a deceleration of $d\omega/dt = -1900$ krad/s is estimated. Multiplying by the local moment of inertia gives a torque density of -0.67 Nm/m³, and assuming the torque is uniform over the island width evaluates to approximately -3 Nm (slightly larger than one tangential neutral beam source on DIII-D). This simple calculation must overestimate the torque from the NTM by a factor of 2, since the plasma remains co-rotating despite zero net injected torque (and the TRANSP [11] calculated absorbed torque is in fact actually slightly counter owing to the edge counter $j \times B$ torques from edge losses), and the intrinsic torque is estimated to be at most 1.5 Nm (Sec. 3). This illustrates part of the challenge of predicting the rotation profile for ITER, because uncertainty in any of the comparatively small torques can have a large impact on the momentum balance.

Interestingly, the overall performance of the discharge was not improved by using additional ECH power to completely suppress the mode, since the total power (NB+ECH) required to achieve the same β_N was the same with or without the mode. Hence, the expected increase in confinement from suppressing the mode is offset by a reduction in confinement associated with the EC power. This appears to be a result of a combination of reducing the T_i/T_e ratio, together with the less favorable deposition of power at large radius. This clearly illustrates a disadvantage on relying on electron cyclotron current drive for mode control in a high gain scenario; it is critical for machine protection to be able to avoid a disruptive locked mode, but the cost in terms of confinement does not make it an especially attractive solution, unless it can be pulsed on periodically to quickly suppress modes as they first appear.

Figure 3 shows the trajectory in β_N -torque space comparing discharges with and without ECH. A region of instability is readily identifiable in cases without ECH (although the 2/1 NTM limit cannot be characterized solely by these two quantities). This is true, independent of whether one ramps the torque down at high β_N (the traditional “high torque startup”), or ramps the β_N up at low torque (the main focus of this work concerning access to the regime). However, with ECH applied, it becomes possible to avoid the 2/1 NTM and push past this barrier of instability, allowing access to higher performance low torque plasmas. In many cases in this data set, the ECH has been aimed to drive current near the $q=2$ surface, although it is not clear whether this is really a critical element in order to

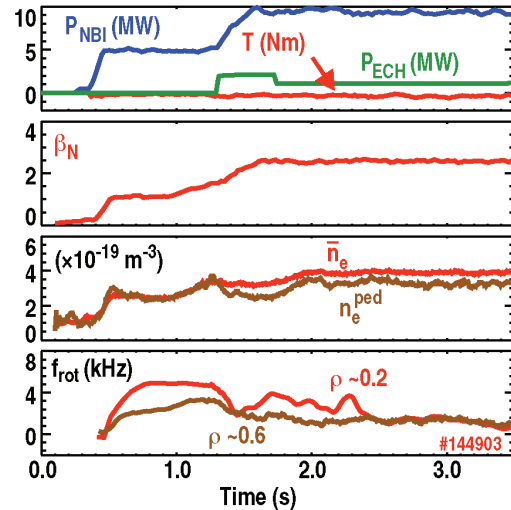


FIG. 2. Advanced inductive discharge produced and sustained with zero net torque at $\beta_N \sim 2.4$ and rotation ~ 1 kHz.

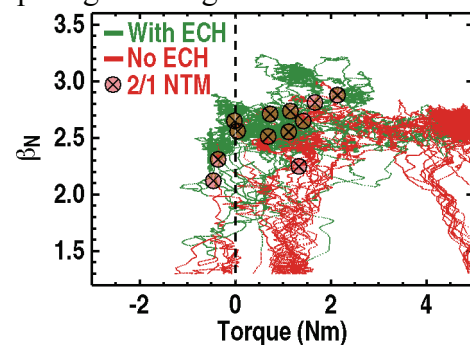


FIG. 3. Trajectories highlight the difficulty in accessing high β_N low torque plasmas without ECH.

gain the benefits of the ECH.

While both theory and experimental evidence have indicated quite rigorous requirements for the alignment of the ECCD to achieve NTM suppression, these experiments did not utilize any form of active tracking of the $q=2$ surface, which is evolving notably particularly during the ramp up to high β , but rather used a broad deposition of the ECH power in the general vicinity of deposition of the ECH power in the general vicinity of $q=2$. In many cases, however, it was noted that the misalignment with the surface was substantial, yet the NTM would remain suppressed. Moreover, in cases such as Fig. 2, where the mode was merely controlled rather than suppressed, the mode amplitude was not seen to vary as the q -surfaces evolved over the course of the discharge, even when substantially better alignment was achieved later in time. Armed with this knowledge, and given the negative impact on the fusion gain associated with off-axis heating, we were motivated to see how far inside the $q=2$ surface we could move the ECH and still suppress the mode. In the discharge represented in Fig. 4, the EC was shifted in closer to the center at $\rho < 0.3$, compared with about 0.6 for the $q=2$ surface. Moreover, in this case, the gyrotrons were re-aimed nominally for heating only with minimal current drive. Somewhat surprisingly, the same beneficial effects from the EC is observed, as can be seen by comparing the discharge in blue with EC to the one in red without, of which the latter immediately encounters a 2/1 NTM at the beginning of the high beta phase. The effect of the EC, even with poor alignment, was quite robust — turning off the EC power when operating in the unstable regions of Fig. 3 would invariably lead to a rapid triggering of the 2/1 NTM. The insensitivity of the NTM control to either the deposition location, or the configuration for heating versus current drive, suggests that the EC is assisting the stability in an additional way to the well-documented technique in which the ECCD replaces the helical deficit in the bootstrap current associated with an island. One possibility is that the EC increases cross-field transport, resulting in flatter profiles and a smaller bootstrap current in the vicinity of the $q=2$ surface (such that the island flattening of the profile is a relatively smaller helical perturbation). However, calculations of the bootstrap current j_{bs} in cases with and without ECH power show only a very modest difference ($j_{bs}=9.6$ A/cm² with ECH compared with $j_{bs}=10.2$ A/cm² without ECH near the time of the mode onset), so this does not appear to be the mechanism either. For now, we simply speculated that the ECH leads to a direct modification of the classical Δ' stability parameter via changes to the conductivity (and thus Ohmic current) and bootstrap current profiles.

Access to lower torque and higher β_N has so far proved challenging without ECH, even though the exact mechanism by which it aids stability is unclear. Other options besides ECH power were explored to try to control the 2/1 NTM. Changes in the formation phase of these low torque startup plasmas, aimed at trying to find a more stable current profile, including the plasma current ramp rate, the timing of the heating and the timing of the L-H transition, did not appear to significantly alter the low torque stability of these plasmas, although this exploration remains far from exhaustive at this stage. One obvious question to address was

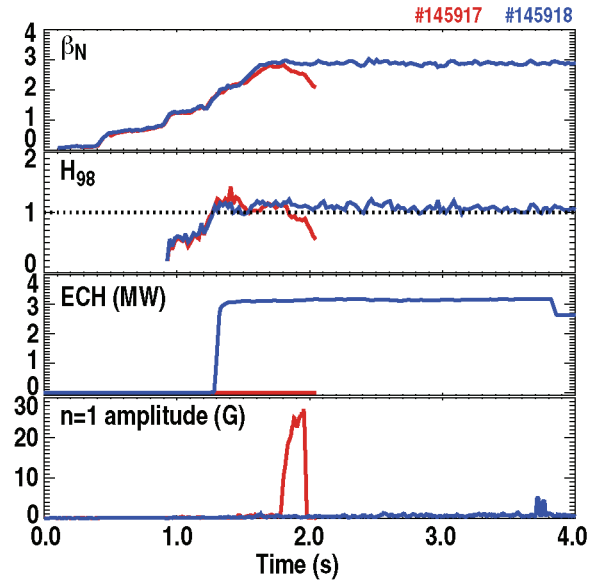


FIG. 4. Comparison of two AI discharges, one using ECH (blue) deposited inside $\rho < 0.3$ (well inside of $q=2$), and the other without ECH (red). The case without ECH rapidly encounters a 2/1 NTM soon after entering the high β_N phase.

whether the 2/1 NTM was being triggered by an uncorrected $n=1$ error field. If this were the case, then lower torque operation should be possible with improved error field correction, which may have obviated the need for ECH. To investigate this, the dynamic error field correction (DEFC) system [12] was used to try to optimize currents in the correction coils to produce the best error field correction. Even though the system converged to a solution using approximately 50% more current in the coils than the standard error field correction algorithm would prescribe (a fairly typical result for high beta H-mode plasmas), there did not appear to be any improved access to low torque using the correction fields determined by the DEFC system (if anything, it was actually slightly worse, judging by the torque level at which the mode struck in a standard torque ramp down shot). From this, it is concluded that the 2/1 NTMs in these plasmas are probably not the result of an uncorrected residual $n=1$ error field. As part of the investigation of the role of the error field, the error field correction was also completely removed. In this case, a considerable impact on the confinement was noticed, with the plasma reaching lower β_N despite using 20% more power than the standard error field correction case. Unfortunately, no further increases in confinement were observed in going from the standard correction to the DEFC solution.

3. Confinement at Low Torque and Rotation

As illustrated dynamically in Fig. 1, the confinement of the advanced inductive regime shows a particular sensitivity to the applied torque and rotation. This is also observed across the set of stationary conditions as shown in Fig. 5(a). Previous modeling with GLF23 [13] has attributed this loss in confinement with an increase in low- k turbulence associated with the reduction in $E \times B$ shear as the rotation is reduced. Analysis of the ion and electron transport indicate a notable increase in the diffusivity profiles of both channels as the rotation is reduced, also represented in Fig. 5 at $\rho=0.8$, with the ion thermal transport showing the largest effect. This basic trend with rotation is observed at all major radii in the data, although it is more pronounced toward the outer half of the plasma, and is also seen when plotted against the applied torque. In this case, we use the rotation is used as a rough means of normalizing the effect of the torque for different densities, plasma currents and toroidal fields in the data.

TGLF modeling of the transport and temperature profiles has been performed for a shot with a torque ramp down, similar to the one shown in Fig. 1. In these simulations, the density and rotation profiles are input from the experiment, and TGLF predicts the thermal transport and ion and electron temperature profiles, using a boundary condition at $\rho \sim 0.84$. The TGLF ion and electron thermal diffusivities, χ_i and χ_e , are overplotted in Fig 5. Qualitatively, TGLF appears to do a reasonable job in reproducing the trend with rotation, and χ_i also shows some quantitative agreement, while χ_e is off by approximately a factor of 2–3. For both ions and electrons, TGLF suggests that most of the transport changes with rotation occur outside of $\rho > 0.6$, with

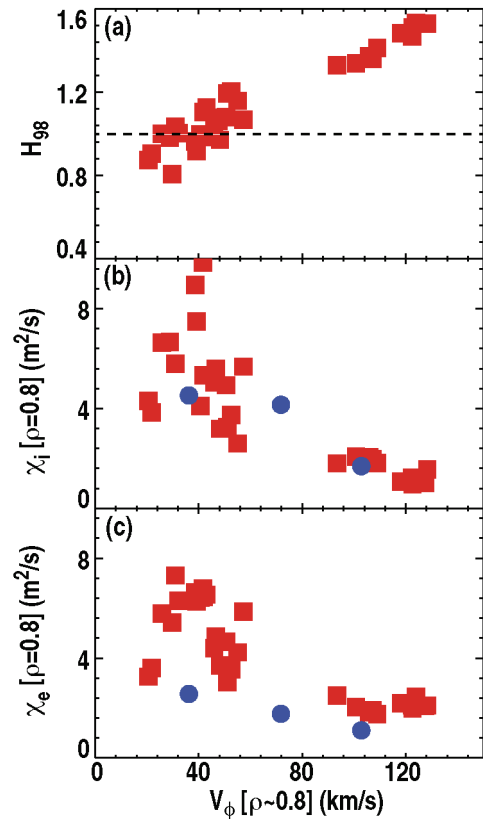


FIG 5. Dependence of (a) H_{98} confinement factor, (b) ion thermal diffusivity and (c) electron thermal diffusivity on rotation (red). Overplotted are predictions from TGLF during a torque rampdown in an AI discharge.

only very modest changes inside this, which is somewhat different than the data, which shows a more uniform increase across the profile. Inside of $\rho < 0.3$, TGLF finds that ETG turbulence completely dominates the electron channel, and the TGLF predicted temperature profiles at high and low rotation are shown in Fig. 6. The substantial missing electron transport leads to a significant overprediction and peaking of the T_e profile compared with the experimental measurement.

The temperature ratio, T_i/T_e ratio appears insensitive to the applied torque, remaining approximately fixed at 1.8 on axis during the torque ramp down. In going from high to low torque in Fig. 1, the injected beam power increases from approximately 5.4 MW to 9.1 MW (prior to the onset of the 2/1 NTM). TRANSP calculations show that approximately 1.3 MW of additional power flows through each of the ion and electron channels, with the remaining 1.1 MW of extra power associated with increased losses from the counter beams (primarily orbit and charge exchange losses).

During torque ramps from high to low rotation in these AI discharges, no major evolution in the q -profile is observed. However, evaluating the current profile evolution is made more complicated due to the sensitivity of the motional Stark effect (MSE) diagnostic to not only the magnetic pitch, but also the radial electric field, which inherently varies with toroidal rotation. Both charge exchange recombination (CER) measurements, as well as co- and ctr-NBI MSE views, have been used to correct for the E_r contribution to the signal. Both approaches agree relatively well, and find that any change to the q -profile is modest, with q_{min} dropping at most $0 < q_{min} < 0.1$. Transport modeling with TGLF demonstrates that such changes in the q -profile cannot account for any of the changes in confinement, with the inferred ion thermal diffusivity essentially unchanged in simulations when the q -profile from a high rotation AI discharge is substituted in for a low rotation case.

One curious observation is the fact that if we start from a low torque advanced inductive discharge and ramp the torque back up to levels typical for co-only NBI discharges, then we do not recover the typical improved performance of rapidly rotating AI plasmas. In particular, it was found that even after the torque has been increased back to 5 Nm, the rotation and rotation shear remain at levels less than half that of a standard AI plasma, and the confinement quality barely changes. This clearly illustrates the path dependence in obtaining high performance discharges.

A consideration for these low torque scenarios is the potential difference between low external torque and low rotation, which may arise due to so-called intrinsic rotation, where the plasma is found to rotate even in the absence of external momentum input. An excellent predictor for the intrinsic drive originating at the edge of the plasma has previously been determined on DIII-D [14], and includes contributions from the turbulent Reynolds stress [15,16] and thermal ion orbit loss [17]. The new advanced inductive discharges have intrinsic

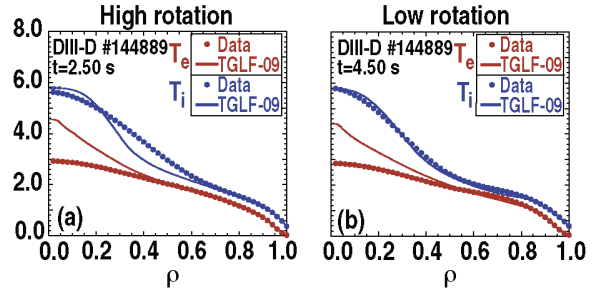


FIG 6. TGLF prediction of ion and electron temperature profiles, and comparison with the experimentally measured quantities, for high rotation (left), and low rotation (right). While the ion temperature prediction is reasonable, the electron temperature is significantly overpredicted in the center.

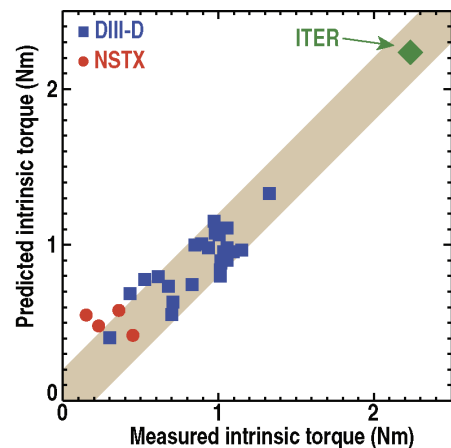


FIG 7. Intrinsic torque measured in high β_N AI discharge, and comparison with scaling in [14]. A prediction for the intrinsic torque on ITER is also shown.

torques that significantly exceed the range of values used in constructing the scaling, in large part due to the higher β_N , but as shown in Fig. 7, still closely follow the previous scaling. There are indications that the same scaling works relatively well for NSTX discharges, which may suggest weak if any ρ^* scaling. This potentially has significant implications for the intrinsic drive in ITER. In particular, if the same scaling holds for ITER, then the intrinsic drive will be very small, about 2 Nm, considerably smaller than even the NBI torque.

The momentum diffusivity computed using TRANSP shows a qualitatively similar behavior with rotation as the thermal channels. However, note that the momentum diffusivity directly computed by TRANSP appears to “roll over”, and even go negative, once the rotation (and hence torque) becomes relatively low. This is an artifact of the comparatively larger error in neglecting the intrinsic torque as the externally driven torque is reduced. If we make an approximate correction to the momentum diffusivity $\chi_\phi^* = (1 + T_{\text{intrinsic}}/T_{\text{NBI}})\chi_\phi$ [18], assuming about 1.5 Nm of intrinsic torque as measurements indicate, this artifact is essentially removed, and the increase in momentum transport with reduced rotation becomes clearer, as illustrated in Fig. 8.

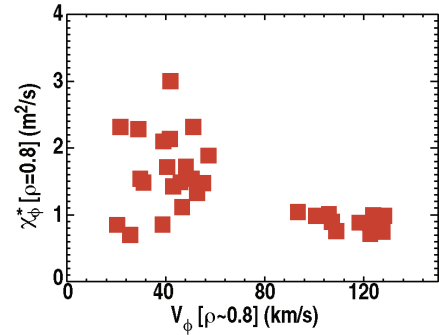


FIG 8. Dependence of momentum diffusivity on toroidal rotation, corrected for approximated intrinsic torque.

4. Access to High Normalized Fusion Performance Discharges with Low Torque

As described in Fig. 2, moderately high $\beta_N \sim 2.5$ advanced inductive discharges have been produced using zero net torque for the maximum duration of the DIII-D counter beams, and required essentially the maximum available balanced neutral beam power. As noted earlier, the use of additional torque free heating from ECH for mode control did not significantly increase the stored energy content. Therefore, to further explore the high β_N limits of the regime at low rotation, it was desirable to relax the torque constraint from 0 Nm, to make more beam power available (DIII-D has 6 co-NBI sources, but only 2 counter-NBI sources). Ideally, one might choose to operate with a rotation level on DIII-D the same as expected on ITER. However, predictions for ITER’s rotation remain relatively uncertain, due to evolving understanding of momentum transport, intrinsic drive and other significant torques on the plasma (e.g. from non-axisymmetric fields). Instead we elected to investigate at an ITER relevant level of injected torque, by requiring that the beam-driven contribution to the rotation on DIII-D is equivalent to that expected for ITER. To estimate this level of torque, we consider simple 0D angular momentum balance, $dL/dt = T_{\text{NBI}} - L/\tau_\phi = 0$ in stationary conditions, where L is the angular momentum, T_{NBI} is the neutral beam torque, and τ_ϕ is the angular momentum confinement time. Note that $L = I\omega$, where I is the moment of inertia of the plasma, and ω the rotation frequency (here taken as a constant for simplicity). Hence, equating ω for DIII-D and ITER, and assuming that $\tau_\phi \approx \tau_E$, one can solve for the torque equivalent on DIII-D as $T_{\text{NBI}}^{\text{DIII-D}} = T_{\text{NBI}}^{\text{ITER}} (I^{\text{DIII-D}}/I^{\text{ITER}}) (\tau_E^{\text{ITER}}/\tau_E^{\text{DIII-D}})$. For ITER scenario 2, $\tau_E^{\text{ITER}} = 3.7$ s, $I^{\text{ITER}} = 1.1 \times 10^{-2}$ Nms² and the total absorbed neutral beam torque for 1 MeV beams has been calculated as $T_{\text{NBI}}^{\text{ITER}} \approx 35$ Nm [19], and for these present DIII-D advanced inductive discharges we have $\tau_E^{\text{DIII-D}} = 0.073$ s and $I^{\text{DIII-D}} = 5.6 \times 10^{-6}$ Nms², then the equivalent torque on DIII-D is estimated to be 0.9 Nm. We therefore opted to constrain the injected torque near 1 Nm (noting that the absorbed torque is typically significantly less).

Advanced inductive discharges approaching the ITER $Q=10$ equivalent, as estimated by the normalized fusion performance parameter $G = \beta_N H_{89}/q_{95}^2$, have been accessed and maintained using net NBI torque down to about 1 Nm. An example of such a discharge is

shown in Fig. 9. The rotation relaxes to a relatively low level under these conditions, yet we maintain β_N above 3 and H_{98} of 1, sustained for the maximum on time duration of the counter NBI system. This translates to a normalized fusion performance of $G \sim 0.35$, compared with approximate $G \sim 0.42$ for ITER's $Q=10$ mission. This advanced inductive discharge operates with $q_{95} \sim 4$, and used approximately 11.4 MW of beam power, and an additional 3.3 MW of ECH deposited at about mid-radius. These discharges were still limited by the available torque-constrained heating power, rather than any upper limit in β_N being encountered. Hence, it is expected that either higher β_N operation, in combination with perhaps higher plasma current, should permit operation at the target G . The temperature ratio in these discharges is relatively close to one outside of about mid-radius, owing to the off-axis deposition of the ECH. However, T_i/T_e remains close to 2 on axis.

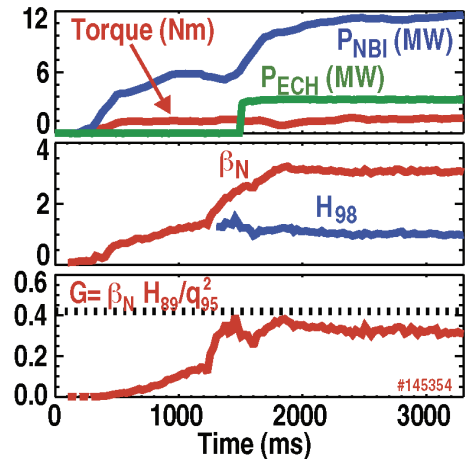


FIG 9. Plasma shot illustrating high normalized fusion performance $G \sim 0.35$ achieved with low torque startup.

5. Conclusions

This recent work demonstrates that high performance advanced inductive discharges can be accessed and sustained with low levels of externally driven torque. Indeed, on DIII-D, using NBI torque that contributes equivalent levels of angular momentum as might be expected from the ITER NBI system, normalized fusion performance has been achieved that approaches ITER $Q=10$ operation. This is achieved with high β_N operation and $q_{95} \sim 4$, in spite of the reduced confinement associated with the lower rotation and torque. The lower confinement appears to affect both ions and electrons equally, and momentum transport is also degraded at low rotation. Although the scenario is extremely robust to locked modes at high torque for this level of fusion performance, in these low rotation conditions we find that the 2/1 NTM is readily destabilized and promptly locks in NBI only heated discharges. The use of ECH at modest levels has proven effective in preventing the 2/1 mode from growing, although it does not appear to be essential that the EC power is deposited to drive current at the $q=2$ surface, as would be expected for standard NTM stabilization.

This work was supported by the US Department of Energy under DE-AC02-09CH11466, DE-FC02-04ER54698, DE-FG02-04ER54761, DE-FG02-08ER85195, and DE-AC52-07NA27344.

References

- [1] STRAIT, E.J., et al., Phys. Rev. Lett. **74** (1995) 2483
- [2] BURRELL, K.H., Phys. Plasmas **4** (1997) 1499
- [3] POLITZER, P.A., et al., Nucl. Fusion **48** (2008) 075001
- [4] WADE, M.R., et al., Nucl. Fusion **45** (2005) 407
- [5] DOYLE, E.J., et al., Nucl. Fusion **50** (2010) 075005
- [6] NAVE, M.F.F. and WESSON, J.A., Nucl. Fusion **30** (1990) 2575
- [7] ZOHN, H., Phys. Plasmas **4** (1997) 3433
- [8] PRATER, R., et al., Nucl. Fusion **47** (2007) 371
- [9] LA HAYE, R.J., et al., Nucl. Fusion **46** (2006) 451
- [10] LA HAYE, R.J., et al., Phys. Plasmas **7** (2000) 3349
- [11] HAWRYLUK, R., Phys. Plasmas Close to Thermonuclear Conditions, B. Coppi, et al., Editor (CEC, Brussels, 1980) Vol. 1, pp. 19–46
- [12] GAROFALO, A.M., et al., Phys. Rev. Lett. **89** (2002) 235001
- [13] KINSEY, J.E., et al., Fusion Sci. Technol. **44** (2003) 763
- [14] SOLOMON, W.M., et al., Nucl. Fusion **51** (2011) 073010

- [15] DOMINGUEZ, R.R and STAEBLER, G.M., Phys. Fluids B **5** (1993) 3876
- [16] GÜRCAN, Ö.D., *et al.*, Phys. Plasmas **14** (2007) 042306
- [17] deGRASSIE, J.S., *et al.*, Nucl. Fusion **49** (2009) 085020
- [18] SOLOMON, W.M., *et al.*, Plasma Phys. Control. Fusion **49** (2007) B313
- [19] BUDNY R.V., *et al.*, Nucl. Fusion **48** (2008) 075005